processes

MDPI

Article

Effect of Inclined Orifice in Air Impingement Freezer on Heat Transfer Characteristics of Steel Strip Surface

Jing Xie [1,2,*], Xilan Luo [1], Jinfeng Wang [1,2] and Yuyan Liu [1]

[1] College of Food Science and Technology, Shanghai Ocean University, Shanghai 201306, China; 2035206@st.shou.edu.cn (X.L.); jenniferwjf@126.com (J.W.); LYY3475506675@126.com (Y.L.)
[2] National Experimental Teaching Demonstration Center for Food Science and Engineering, Shanghai Ocean University, Shanghai 201306, China
* Correspondence: jxie@shou.edu.cn

Abstract: In order to improve the heat transfer characteristics of the air impingement freezer, an impingement freezer experimental table was designed as the research object in this paper. Numerical simulation technology was used to simulate the impingement freezer experimental table on the basis of test verification. When the other structural parameters in the impingement freezer experimental table were constant, the effect of the inclination angle of the orifice plate (θ = 60°, 65°, 70°, 75°, 80°, 85°, and 90°) on the heat transfer characteristics of a steel strip surface was analyzed by two aspects, the average Nusselt number and the heat transfer uniformity. The results showed that with the increase in the inclination angle of the orifice plate ($60° \leq \theta \leq 90°$), the average Nusselt number of the steel strip surface was increased by 19.39%, and the heat transfer uniformity index was decreased by 33.69%. When θ = 90°, the average Nusselt number on steel strip was the maximum, which was 263.68, and the heat transfer uniformity index was the minimum, which was 0.2039. Therefore, the heat transfer intensity and heat transfer uniformity in the air impingement freezer could be improved when the inclination angle of the orifice plates was 90°. This helps to improve the output of the air impingement freezer, reduce energy consumption, and improve the quality of frozen food.

Keywords: jet impact; freezer; inclination angle; Nusselt number; uniformity of heat transfer

Citation: Xie, J.; Luo, X.; Wang, J.; Liu, Y. Effect of Inclined Orifice in Air Impingement Freezer on Heat Transfer Characteristics of Steel Strip Surface. *Processes* **2023**, *11*, 2410. https://doi.org/10.3390/pr11082410

Academic Editors: Paolo Blecich and Tomislav Mrakovčić

Received: 11 July 2023
Revised: 3 August 2023
Accepted: 7 August 2023
Published: 10 August 2023

1. Introduction

An impinging jet is a common way to enhance heat and mass transfer in heating, cooling, and drying process [1,2]; it is encountered in many industrial processes such as gas turbine cooling, metal annealing, cooling the blades of aeroengines, and cooling electronic equipment [3,4]. In a freezer, this technology directs high-velocity air jets to break the insulating boundary layer that surrounds the products to be frozen, thereby enhancing the heat transfer and greatly reducing the freezing time to ensure food safety and quality [5–7]. The inclination angle of the impinging jet is one of the main factors affecting heat transfer [8]. Dhruw et al. [9] studied the local heat transfer characteristics due to an inclined jet on the longitudinal vertical and intercentric axial location at different orientations. It was observed that the peak Nu_{ave} increased with increasing inclination of the nozzle jet (15° to 75°) when Re = 34,000, and the highest local Nu_{ave} peak appeared at the jet inclination angle θ = 75°. This was the same as the experimental results of Ingole et al. [10], who conducted an experimental study with Re of 2000 to 20,000, the ratio of nozzle to target surface distance to nozzle diameter (H/D) of 0.5 to 6.8, and the impact jet inclination angle of 15° to 75°. It was found that a 15° tilted jet caused most of the fluid to detach from the target surface, the Nu_{ave} of the target surface was low at this time, and the inclination jet angles of 45° and 60° were best for heat transfer on the target surface. Attalla et al. [11] investigated the heat transfer characteristics of the target surface at Re of 10,000 to 40,000, the ratio of nozzle to target surface distance to nozzle diameter (H/D) of 2 to 8, the ratio of nozzle clearance to nozzle diameter (S/D) of 2 to 8, and jet inclination

angle of 0° to 60°. The experimental results showed that the target surface Nu_{ave} was the largest when the slope of the jet was in the range of 10° to 20°. In summary, the inclination of the jet affects the heat transfer intensity of the target surface. However, most of the existing literature mainly focuses on the magnitude of the target surface Nu_{ave} but ignores the heat transfer uniformity of the target surface, which is also one of the important factors affecting the quality of frozen food in freezers [12,13], and therefore should not be ignored in this study. The heat transfer uniformity of the target surface can be enhanced by certain methods. Wen et al. [14] changed the shape of the pressure outlet of the vehicle by adding baffles, reducing the final target surface inhomogeneity coefficient by 39.70% and effectively improving the heat transfer uniformity.

Numerical simulation can simulate complex working conditions and visualize some detailed information, which helps to achieve a deep understanding of the airflow field characteristics and heat transfer properties of the jet impingement cooling process [15]. Therefore, this paper obtained from pre-experiments that the heat transfer strength of the steel strip surface was stronger in the range of θ from 60° to 90°. Based on the experimental validation of the computational fluid dynamics (CFD) numerical simulation model, the orifice plate was inclined to achieve the inclined jet. The inclination angle of the orifice plate is the same as the inclination angle of the jet. This paper mainly investigates the effect of the inclination angle of the orifice plate on the heat transfer characteristics of the steel strip surface in the impact freezer test rig. Then, from two perspectives—the average Nusslet number of the target surface and the heat transfer uniformity index—the optimal inclination angle of the orifice plate is found, which eventually aims to provide a theoretical basis for the optimal design of the new upper and lower impact type freezer.

2. Materials and Methods

2.1. Building a Physical Model

A model of the impact freezer test bench is illustrated in Figure 1. The basic rationale for this is: the cooling air is guided by a centrifugal fan into the plenum box of the test bench, where it is directed through the upper and lower 2 orifice plates to form an impinging jet onto the surface of the strip. Sequentially, the cold is transferred to the steel strip through the two heat transfer methods of convection and conduction. Then, it flows in a defined channel and is discharged through the pressure outlet at the very end. The size of the plenum box is 300 mm × 300 mm × 500 mm, and the size of the orifice plate is 300 mm × 300 mm × 2 mm. Oval nozzle, the aspect ratio AR = 1.95, the nozzle gap S = 33.8 mm, the number of nozzle rows N = 8, and the distance from nozzle to steel strip H = 22.8 mm. The change in the internal flow field of this equipment was found to be the same as that of the impact tunnel freezing equipment produced by Nantong Sifang Cold Chain Equipment Co [16]. This experiment takes the orifice plate as the research object. The effects of different orifice plate inclination angles θ on the surface heat transfer characteristics of steel strip were compared. Figure 2 shows the orifice plate model. The orifice plate inclination θ is the angle formed by the impinging jet and the OX-axis, and there are vertical and inclined jets by an inclination angle [17]. The θ values are in the range of 0° to 90, and the jet with an inclination of 90° is usually referred to as a perpendicular jet [10].

2.2. Grid Division

The physical model was meshed using ANSYS 15.0 software, and the grid around the nozzle was appropriately encrypted and refined to improve the computational accuracy [18,19]. Taking the orifice plate inclination angle of 90° as an example: the minimum size of the encrypted grid at the nozzle is 0.3269 m, the number of nodes in the computational domain of the model is 643,905, and the number of grid cells is 2,428,986. The numerical simulation result is shown in Figure 3.

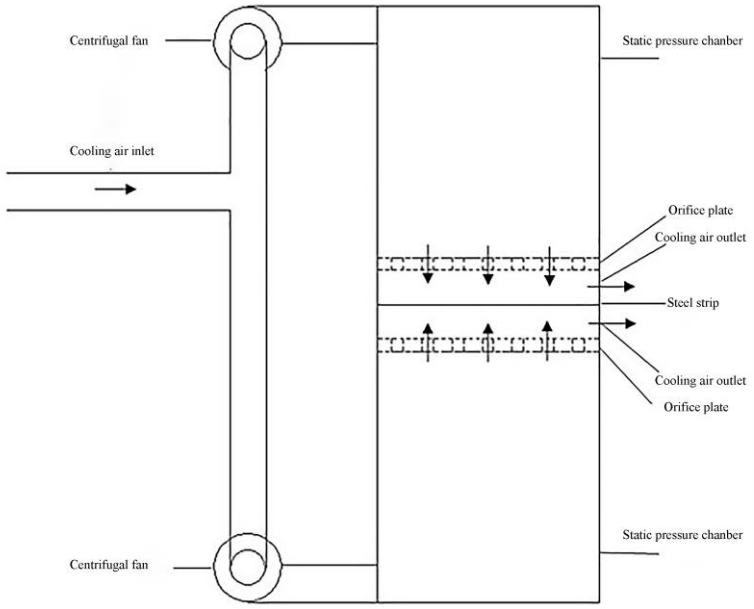

Figure 1. Model of impacting freezing experiment table.

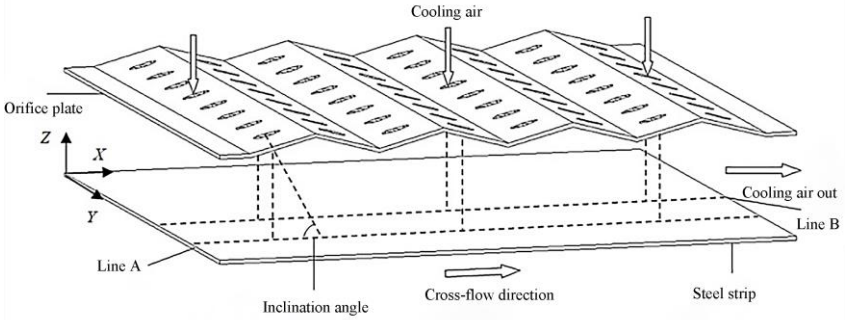

Figure 2. Model of orifice plate.

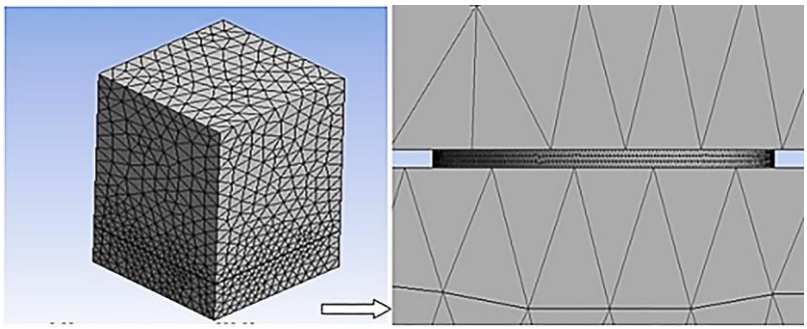

Figure 3. Mesh encryption.

2.3. Simulation Equations and Boundary Condition Settings

The conservation equations of the computational model were solved using the ANSYS-Fluent code.

The fluid medium for this simulation is air. It is assumed that: (1) the walls of the plenum box chamber are adiabatic and non-slip [20,21], (2) the air is an incompressible fluid [22,23], and (3) the flow field inside the impinging freezer test bench is in a steady state [24].

The test method of Wang et al. [21] was referred to and suitably modified. The model was calculated using the k-ε equation and the SIMPLE (Semi-Implicit Method for Pressure Linked Equation) algorithm [25,26]. The continuity equation, momentum equation, and energy equation are jointly solved during numerical simulation [27]. Inlet pressure is used

as the inlet boundary condition and outlet pressure as the outlet boundary condition. This setup is more realistic and more accurate in its calculations. The inlet pressure P_{in} was set to 250 Pa, the outlet pressure P_{out} was set to 0 Pa, the cooling air inlet temperature was taken to be 230 K, the cooling air outlet temperature was taken to be 235 K, and the mass flow rate at the cooling air inlet was 0.0644 kg/s. The steel strip is set as a wall and the thermal conductivity is 16.3 W/(m·°C).

2.4. Definition of Parameters

To facilitate the analysis of the heat transfer strength at different locations on the steel strip, lines A and B were considered on the surface of the strip (as in Figure 2) [28]. Line A corresponds to the line directly below the center of each row of nozzles; there are eight rows of nozzles in total, so they are lines A1, A2, . . ., A8, respectively. Line B corresponds to the center line of the nozzle gap directly below the nozzle gap; there are seven rows of nozzle gaps, so they are lines B1, B2, . . ., B7. The formula for the average Nusslet number on line A and line B is:

$$Nu_{\mathrm{aveA}} = \frac{Nu_{\mathrm{A1}} + Nu_{\mathrm{A2}} + \cdots + Nu_{\mathrm{A8}}}{8} \tag{1}$$

$$Nu_{\mathrm{aveB}} = \frac{Nu_{\mathrm{B1}} + Nu_{82} + \cdots + Nu_{7}}{7} \tag{2}$$

In the formula, Nu_{aveA} is the average Nusselt number on line A; Nu_{Ai} (i = 1, 2, $\cdots$, 8) is the number of Nusserl's directly below the center of each nozzle line; Nu_{aveB} is the average Nusselt number on line B; Nu_{Bi} (j = 1, 2, $\cdots$, 7) is the Nusselt number directly below the center line of each nozzle gap in each line.

The steel strip surface heat transfer uniformity index η represents the difference in the Nusslet number at different locations on the strip surface. The uniformity of the steel strip surface increases as the η decreases. This is calculated as follows [14,29,30]:

$$\eta = \frac{\sigma_{Nu}}{Nu_{\mathrm{ave}}} \tag{3}$$

In the formula, σ_{Nu} is the standard deviation of the local Nusslet number of the strip surface, and Nu_{ave} is the average Nusslet number of the strip surface.

2.5. Experimental Verification

Under the same numerical simulation conditions, Xie et al. [16] experimentally measured the absolute velocity in the OZ-direction of each nozzle exit along the OX-axis when the orifice plate of the impact freezer experimental table was inclined at an angle of 90°. They found that the error between the numerical simulation results and the experimental measurement results were in the range of 2.83% to 4.95%. Therefore, the numerical simulations in this paper are plausible for an impact freezer test bench [31].

3. Results

The N_u distribution on the steel strip surface for different orifice plate inclination angles is shown in Figure 4. As the orifice plate inclination angle θ increases from 60° to 90°, the steel strip surface N_u increases in the upstream area away from the pressure outlet and increases in the nozzles in the 1st, 3rd, 5th, and 7th columns along the OX-axis. The local N_u distribution of line A and line B for different orifice plate inclination angles is shown in Figure 5. From Figure 5, it can be seen that when the orifice plate inclination angle θ is 60° and 70°, the 1st, 3rd, 5th, and 7th columns of nozzles of the strip surface N_u number peak are lower than the 2nd, 4th, 6th, 8th columns of nozzles of the strip surface N_u number peak, respectively. Additionally, the peak N_u on the strip surface gradually increases along the OX-axis. However, when the orifice plate inclination angle θ was 80° or 90°, there was little difference in the peak N_u number of the steel strip surface in each

column of nozzles. When the orifice plate inclination angle θ was 60°, 70°, 80°, or 90° for line A, the difference between the maximum and minimum (the range) values of local N_u on the steel strip surface gradually decreased to 359, 258, 254, and 206, respectively; and for line B, the range of local N_u on the steel strip surface also gradually decreased to 172, 194, 163, and 113, respectively. This shows that with the increase in the inclination angle of the orifice plate ($60° \leq \theta \leq 90°$), the localized N_u distribution at each position on the surface of the steel strip is more uniform, and the value of η is small.

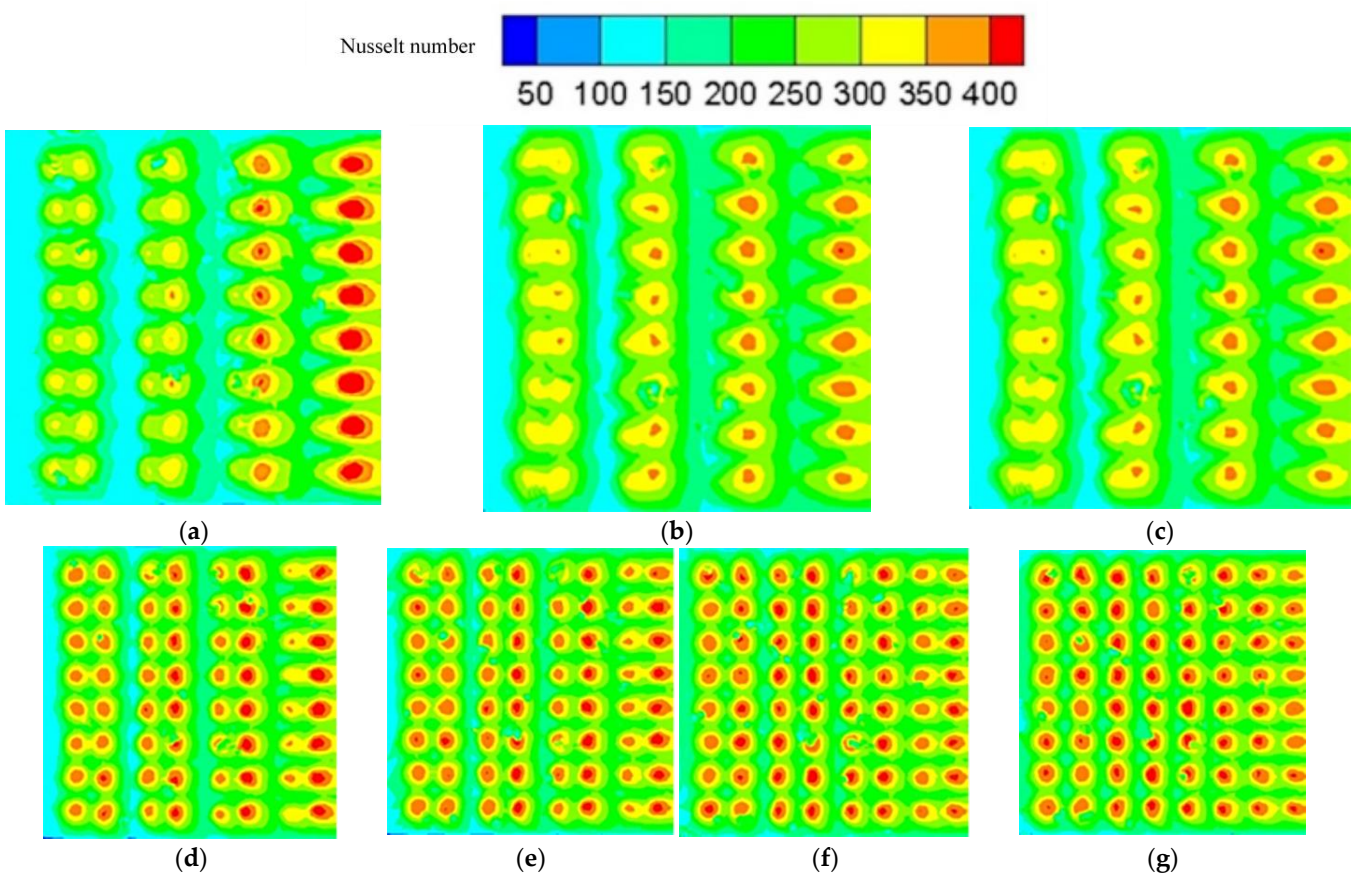

Figure 4. Nusselt number distribution on the steel strip at different inclination angles of orifice plate. (**a**) θ = 60°; (**b**) θ = 65°; (**c**) θ = 70°; (**d**) θ = 75°; (**e**) θ = 80°; (**f**) θ = 85°; (**g**) θ = 90°.

The average Nu_{ave} number distribution of line A and line B for different orifice plate inclination angles is shown in Figure 6a. As can be seen from Figure 6, when the angle of inclination of the orifice plate θ increases from 60° to 90°, the Nu_{ave} of both line A and line B follow an increasing trend, rising by 16.40% and 20.37% respectively, with a larger rise in Nu_{ave} for line B. The average N_u number is the average of Nu_{aveA} and Nu_{aveB}. The surface Nu_{ave} of the steel strip for different orifice plate inclination angles is shown in Figure 6b. As θ increases from 60° to 90°, the strip surface Nu_{ave} increases from 220.86 to 263.68, an increase of 19.39%. When θ = 90°, the steel strip surface Nu_{ave} reaches its maximum. This means that the surface of the strip has the highest heat transfer strength and therefore the quickest freezing time for the food [32]. It also means that when the total output of the freezer is a certain amount, it is the most efficient and uses the least amount of energy. Beitelmal et al. [8] also showed that the heat transfer intensity of the target surface increases with the inclination angle of the impinging jet. Surendra found that when the jets are orthogonal, the gravitational force also promotes the jet impact to hit the disc with more energy, thus increasing the heat transfer coefficient [33].

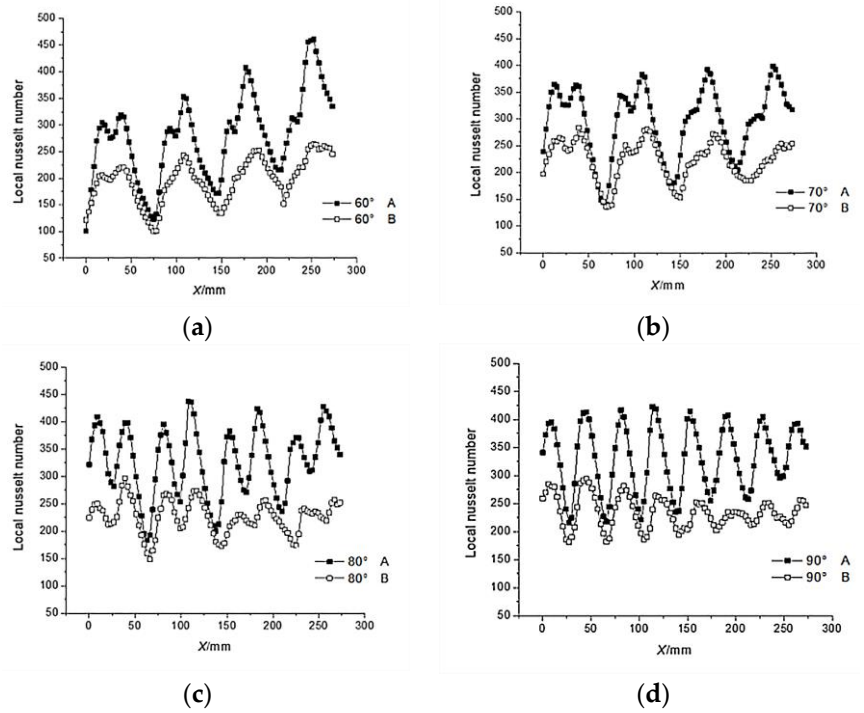

Figure 5. Local Nusselt number distribution on line A and line B at different inclination angles of orifice plate. (**a**) θ = 60°; (**b**) θ = 70°; (**c**) θ = 80°; (**d**) θ = 90°.

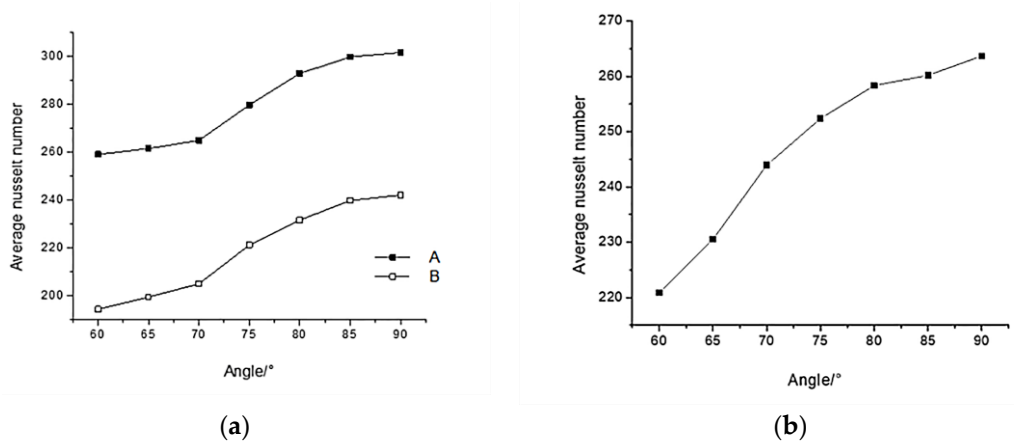

Figure 6. Average Nusselt number at different inclination angles of orifice plate: (**a**) on line A and line B; (**b**) on the steel strip.

The values of the heat transfer uniformity index η on the steel strip surface for different orifice plate inclination angles are shown in Figure 7. As can be seen in Figure 7, when θ was increased from 60° to 90°, the value of the strip surface uniformity index η decreased from 0.3075 to 0.2039, a total reduction of 33.69%. When θ = 90°, the steel strip surface uniformity index η reached a minimum value. This means that the surface heat transfer uniformity of the steel strip is the best.

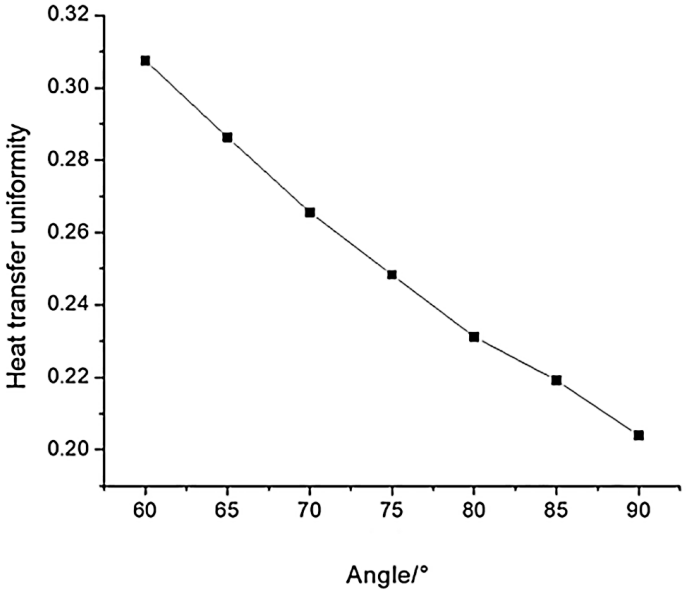

Figure 7. Uniformity of heat transfer on the steel strip at different inclination angles of orifice plate.

4. Discussion

Transverse flow is the flow of fluid in the vertical direction of the impact jet, which is one of the important factors affecting the heat transfer characteristics of the impact jet. Transverse flow can deflect the impact direction of the jet, resulting in a reduction in the velocity of the direct jet impact on the steel strip surface. Therefore, the transverse flow effect is not conducive to the internal heat exchange of the freezer [20,34,35]. When the frozen product in the freezer is shrimp, they are subjected to transverse flow wind velocity at 10 mm above the steel belt during the freezing process [24]. Due to the fact that the general placement height of frozen products during the freezing process is about 10 mm, we considered 10 mm from the surface of the steel belt for our analysis. As shown in Figure 8, when θ increases from 60° to 90°, the transverse flow wind velocity at 10 mm above the strip decreases from 3.97 m/s to 2.56 m/s, a reduction of 35.55%. Thus, the Nu_{ave} of the steel strip surface increases, and the heat transfer properties of the strip surface are enhanced in the transverse flow direction. A similar conclusion was reached in a study by Katti et al. [14], where the heat transfer effect on the target surface increased as the transverse flow effect in the channel decreased. Additionally, with the increase in airflow velocity in the transverse direction of the orifice plate, the frozen products are less likely to flow, which is beneficial to the safe and effective processing of frozen products.

Figure 9 shows the absolute velocity in the OZ-direction at 10 mm of the steel strip surface for different orifice plate inclination angles. When θ = 60°, 75°, and 90°, the velocity ranges were 6.43, 4.89, and 1.37, respectively, and the absolute velocity fluctuation in the Z-direction at 10 mm of the steel strip surface becomes slower. When θ = 60° and 75°, the absolute velocity in the Z direction at 10 mm from the surface of the nozzle strip is lower in columns 1, 3, 5, and 7 than in columns 2, 4, 6, and 8, respectively. When θ = 90°, the absolute velocity in the z-direction at 10 mm from the surface of the strip in each column of nozzles did not differ much and tended to rise. This indicates that as the orifice plate inclination angle θ increases ($60° \leq \theta \leq 90°$), the absolute velocity range in the Z direction at 10 mm on the surface of the steel strip of each column of nozzles gradually decreases, and the N_u range on the surface of the steel strip of each column of nozzles decreases. The value of η responds to the variability of N_u at each position on the surface of the steel strip. The smaller the value of η, the more uniform the heat transfer on the surface of the steel strip, i.e., the uniformity of heat transfer on the surface of the steel strip is improved.

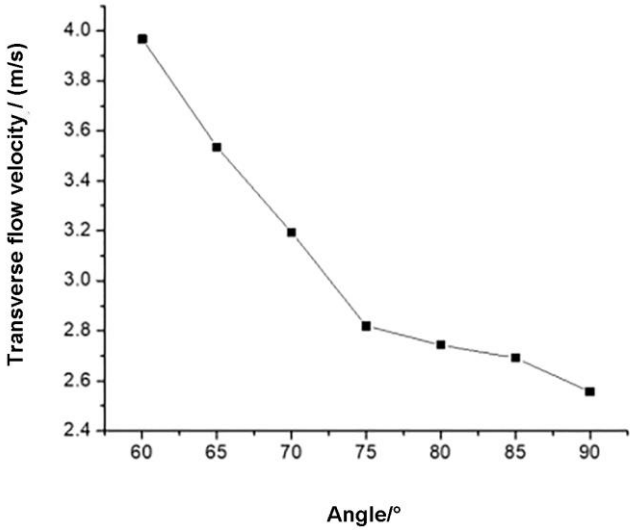

Figure 8. Transverse flow velocity distribution at 10 mm above steel strip surface at different inclination angles of orifice plate.

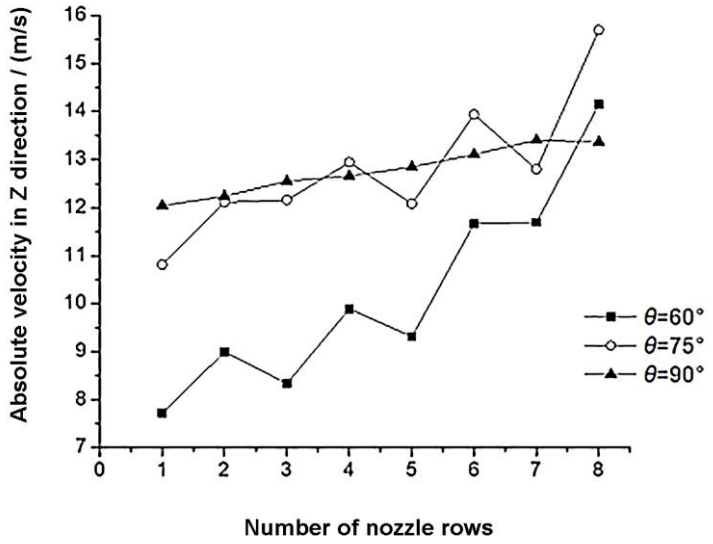

Figure 9. Absolute velocity distribution at 10 mm above steel strip surface in Z direction at different inclination angles of orifice plate.

The orifice plate outlet airflow vector diagram for the three inclination angles is shown in Figure 10. In the figure, the left nozzle is the 3rd column nozzle and the right nozzle is the 4th column nozzle. Transverse flow can be formed by the accumulation of jets away from the pressure outlet, so the direction of transverse flow is from left to right. It can be seen from Figure 10 that when the orifice plate is inclined at angle θ = 60° and 75°, the air flow at the exit of the 3rd column nozzle flows down to the right. The air flow in the OX-axis direction is the same as in the transverse flow direction, which increases the transverse flow effect to a certain extent and reduces the heat transfer strength of the strip surface in the third row of nozzles. The air flow at the exit of the nozzle in column 4 is to the lower left, and in the OX-axis direction it is opposite to the transverse flow direction. The jet is deflected to the right by the transverse flow, which reduces the angle between the jet and the OZ-axis, and increases the velocity in the OZ-direction above the surface of the strip in the fourth row of nozzles. Overall, the heat transfer intensity of the steel strip surface of the nozzles in 2nd, 4th, 6th, and 8th columns is always higher than that of the nozzles in 1st, 3rd, 5th, and 7th columns, respectively. Therefore, the index of non-uniform heat transfer on the steel strip surface is

large. When the orifice plate inclination angle θ = 90 °, the airflow at the nozzle outlet is along the OZ-axis direction to act directly on the surface of the steel strip. Although some crossflow accumulates in the upstream area away from the pressure outlet, it has less of a transverse flow effect than other orifice plates inclination angles. Therefore, the heat transfer strength of the steel strip surface is stronger when θ = 90°.

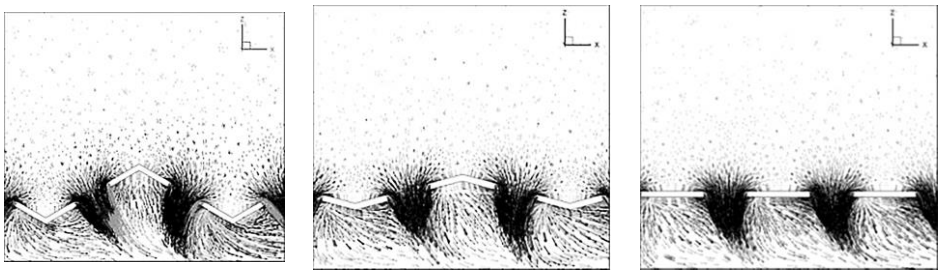

(**a**) (**b**) (**c**)

Figure 10. Flow vector diagram of nozzle outlet. (**a**) θ = 60°; (**b**) θ = 75°; (**c**) θ = 90°.

This is important to reduce the freezing time of food, increase the production capacity of the freezer, and save energy. When θ = 90 °, the airflow direction at the exit of each column nozzle is the same, and its impact on the surface of the steel strip is the same. Therefore, the heat transfer uniformity index on the surface of the steel strip is small, i.e., the airflow in the channel is more evenly distributed. This is important to improve the freezing uniformity and the quality of frozen food.

5. Conclusions

The object of study in this paper is the orifice plate of the impact freezing experimental bench. Using the average Nu_{ave} of the target surface and the heat transfer uniformity index, the effect of the impact jet on the heat transfer characteristics of the target surface when the orifice plate tilt angle θ was 60°, 65°, 70°, 75°, 80°, 85°, and 90° was investigated, and the following conclusions were obtained:

(1) When θ increases from 60° to 90°, the Nu_{ave} of the steel strip surface increases from 220.86 to 263.68, an increase of 19.39%. When θ = 90°, the Nu_{ave} on the surface reaches the maximum, which is conducive to increasing the production capacity of the freezer and reducing energy consumption.

(2) During the increase of θ from 60° to 90°, the steel strip surface uniformity index η decreases from 0.3075 to 0.2039, a decrease of 33.69%. When θ = 90°, the steel belt surface uniformity index η value reaches the minimum, and the uniformity of heat transfer is the best, which is conducive to improving the quality of frozen food.

(3) In summary, when θ = 90°, which is the optimum angle of inclination of the orifice plate, the steel strip surface average Nu_{ave} is the largest and the heat transfer uniformity index η value is the smallest.

The above study suggests that when we design the orifice plate of the up-and-down impact freezing machine, θ should be within the range of 0° to 90°, with a vertical jet inclination angle of preferably 90°; in this condition, the surface heat transfer uniformity of the steel strip is relatively improved, thus improving the quality of the frozen food.

Author Contributions: Conceptualization, X.L. and Y.L.; methodology, X.L.; software, X.L.; validation, X.L.; formal analysis, X.L.; investigation, X.L.; resources, J.W. and J.X.; data curation, Y.L.; writing—original draft preparation, X.L.; writing—review and editing, X.L. and Y.L.; supervision, J.X.; project administration, J.X.; funding acquisition, J.X. All authors have read and agreed to the published version of the manuscript.

Funding: This research was funded by the National Key R&D Program of China, grant number 2019YFD0901604; Science and Technology Innovation Action Plan of the Shanghai Science and

Technology Commission, grant number 19DZ1207503; and the Public Service Platform Project of the Shanghai Science and Technology Commission, grant number 20DZ2292200.

Data Availability Statement: All data are available within the manuscript.

Acknowledgments: The authors gratefully acknowledge the support of Xie Jing in this research.

Conflicts of Interest: The authors declare no conflict of interest.

References

1. Lee, J.; Lee, S.J. The effect of nozzle configuration on stagnation region heat transfer enhancement of axisymmetric jet impingement. *Int. J. Heat Mass Transf.* **2000**, *43*, 3497–3509. [CrossRef]
2. Ansu, U.; Godi, S.C.; Pattamatta, A.; Balaji, C. Experimental Investigation of the Inlet Condition on Jet Impingement Heat Transfer Using Liquid Crystal Thermography. *Exp. Therm. Fluid Sci.* **2017**, *80*, 363–375. [CrossRef]
3. Carlomngao, G.M.; Ianiro, A. Thermo-fluid-dynamics of submerged jets impinging at short nozzle-to-plate distance: A review. *Exp. Therm. Fluid Sci.* **2014**, *58*, 15–35.
4. Wang, L.; Feng, L.H.; XU, Y.; Xu, Y. Experimental investigation on flow characteristics and unsteady heat transfer of noncircular impinging synthetic jets. *Int. J. Heat Mass Transf.* **2022**, *190*, 122760. [CrossRef]
5. Kim, Y.H.; Lee, D.H.; Han, S.H. Investigation of impingement surface geometry effects on heat transfer in a laminar confined impinging slot jet. *Int. J. Heat Mass Transf.* **2017**, *115*, 347–353. [CrossRef]
6. Tang, Z.G.; Liu, Q.Q.; Li, H.; Min, X.T. Numerical simulation of heat transfer characteristics of jet impingement with a novel single cone heat sink. *Appl. Therm. Eng.* **2017**, *127*, 906–914. [CrossRef]
7. Luo, D.; Wu, J.; Ma, Z.; Tang, P.P.; Liao, X.J. Production of high sensory quality Shiitake mushroom (*Lentinus edodes*) by pulsed airimpingement jet drying (AID) technique. *Food Chem.* **2021**, *341*, 128290. [CrossRef] [PubMed]
8. Choo, K.; Kang, T.Y.; Kim, S.J. The effect of inclination on impinging jets at small nozzle-to-plate spacing. *Int. J. Heat Mass Transf.* **2012**, *55*, 3327–3334. [CrossRef]
9. Dhrug, L.; Kothadia, H.B.; Kumar, R.A. Investigation of local heat transfer from a flat plate impinged by an inclined circular jet. *Int. J. Therm. Sci.* **2023**, *184*, 108027.
10. Ingole, S.B.; Sundaram, K.K. Experimental average Nusselt number characteristics with inclined non-confined jet impingement of air for cooling application. *Exp. Therm. Fluid Sci.* **2016**, *77*, 124–131. [CrossRef]
11. Attalla, M.; Maghrabie, H.M.; Specht, E. Effect of inclination angle of a pair of air jets on heat transfer into the flat surface. *Exp. Therm. Fluid Sci.* **2017**, *85*, 85–94. [CrossRef]
12. Li, Y.; Li, F.; Tang, J.; Zhang, R.Y.; Wang, Y.F.; Koral, T.; Jiao, Y. Radio frequency tempering uniformity investigation of frozen beef with various shapes and sizes. *Innov. Food Sci. Emerg. Technol.* **2018**, *48*, 42–55. [CrossRef]
13. Li, D.; Zhu, Z.; Sun, D.W. Effects of freezing on cell structure of fresh cellular food materials: A review. *Trends Food Sci. Technol.* **2018**, *75*, 46–55. [CrossRef]
14. Wen, Z.X.; He, Y.L.; Ma, Z. Effects of nozzle arrangement on uniformity of multiple impinging jets heat transfer in a fast cooling simulation device. *Comput. Fluids* **2018**, *164*, 83–93. [CrossRef]
15. Zhao, B.; Tang, W.S.; Wang, Y.P.; Liu, X.Y.; Jin, R.N. Simulation analysis of the effect of oblique jet on the heat transfer characteristics of the wall. *Machinery* **2022**, *49*, 1–8.
16. Xie, J.; Liu, Y.Y.; Wang, J.F. Effects of nozzle structures of air impinging freezer on heat transfer characteristics of steel strip surface. *Trans. Chin. Soc. Agric. Eng.* **2018**, *34*, 292–298.
17. Mao, J.Y.; Si, J.H.; Chen, J.Q.; Li, G.D.; Wang, X.K. Experimental investigation on sand bed scour by an oblique planar water jet at varying impinging angles. *Ocean. Eng.* **2023**, *279*, 114526. [CrossRef]
18. Xu, L.; Jin, L.; Ma, Y.; Gao, J.M.; Li, Y.L. Numerical study on heat transfer by swirling impinging jets issuing from a screw-thread nozzle. *Int. J. Heat Mass Transf.* **2017**, *115*, 232–237. [CrossRef]
19. Guan, T.; Zhang, J.Z.; Shan, Y. Convective heat transfer by a row of tab-excited impinging jets on a wedge-shaped concave surface. *Int. J. Therm. Sci.* **2016**, *100*, 37–53. [CrossRef]
20. Chen, L.; Brakmann, R.; Weigand, B.; Rodriguez, J.; Crawford, M.; Poser, R. Experimental and numerical heat transfer investigation of an impingement jet array with V-ribs on the target plate and on the impingement plate. *Int. J. Heat Fluid Flow* **2017**, *68*, 126–138. [CrossRef]
21. Wang, J.F.; Li, W.J.; Xie, J.; Yang, D.Z.; Liu, Y.Y.; Lu, W.H.; Yang, X.Y. Influence of two nozzle structures on the flow field and heat transfer characteristics of impinging freezer. *Food Mach.* **2017**, *33*, 80–85+90.
22. Zhu, X.W.; Zhu, L.; Zhao, J.Q. An in-depth analysis of conjugate heat transfer process of impingement jet. *Int. J. Heat Mass Transf.* **2017**, *104*, 1259–1267. [CrossRef]
23. Singh, D.; Premachandran, B.; Kohli, S. Effect of nozzle shape on jet impingement heat transfer from a circular cylinder. *Int. J. Therm. Sci.* **2015**, *96*, 45–69. [CrossRef]
24. Li, Y.; Li, B.; Qi, F.S.; Sherman, C.P. Flow and heat transfer of parallel multiple jets obliquely impinging on a flat surface. *Appl. Therm. Eng.* **2018**, *133*, 588–603. [CrossRef]

25. Hou, Y.; Tao, Y.; Huai, X.L.; Zou, Y.; Sun, D.L. Numerical simulation of multi-nozzle spray cooling heat transfer. *Int. J. Therm. Sci.* **2018**, *125*, 81–88. [CrossRef]
26. Rahman, M.M.; Liu, W.C.; Lv, M.; Pan, H.C. Exploring SIMPLE algorithm for all speeds. *Ain Shams Eng. J.* **2023**, *14*, 101854. [CrossRef]
27. Attalla, M.; Maghrabie, H.M.; Qayyum, A.; Adnan, G.; Specht, E. Influence of the nozzle shape on heat transfer uniformity for in-line array of impinging air jets. *Appl. Therm. Eng.* **2017**, *120*, 160–169. [CrossRef]
28. Li, H.H.; Chen, H.Y.; Cui, Z.W. Numerical simulation on effect of tip clearance between screw flight and barrel on performance of food melt conveying section in single screw extruder for expanding. *Food Mach.* **2016**, *32*, 68–72+76.
29. Subasi, A.; Sahin, B.; Kaymaz, I. Multi-objective optimization of a honeycomb heat sink using Response Surface Method. *Int. J. Heat Mass Transf.* **2016**, *101*, 295–302. [CrossRef]
30. Ma, C.; Yan, C.; Cao, X.W.; Wen, Z.X.; He, Y.L. Numerical study of the heat transfer uniformity problem of an array of air jets. *J. Eng. Thermophys.* **2016**, *37*, 2378–2384.
31. Chen, L.Q.; Zhang, D.; Chen, W.W. Numerical simulation and experiments of two-phase flow in splitter gears based on fluid-solid coupling. *Trans. Chin. Soc. Agric. Eng.* **2014**, *30*, 54–61.
32. Zhang, Z.; Xie, J. Numerical simulation of the flow and temperature fields in a quick-freezing unit with upper and lower air-vented plates. *J. Refrig.* **2009**, *30*, 36–40.
33. Barewar, S.D.; Joshi, M.; Sharma, P.O.; Kalos, P.S.; Bakthavatchalam, B.; Chougule, S.S.; Habib, K.; Saha, S.K. Optimization of jet impingement heat transfer: Optimization of jet impingement heat transfer: A review on advanced techniques and parameters. *Therm. Sci. Eng. Prog.* **2023**, *39*, 101697. [CrossRef]
34. Nuntadusit, C.; Wae-Hayee, M.; Tekasakul, P.; Eiamsaard, S. Local heat transfer characteristics of array impinging jets from elongated orifices. *Int. Commun. Heat Mass Transf.* **2012**, *39*, 1154–1164. [CrossRef]
35. Katti, V.; Prabhu, S.V. Influence of streamwise pitch on local heat transfer distribution for in-line arrays of circular jets with spent air flow in two opposite directions. *Exp. Heat Transf.* **2009**, *22*, 228–256. [CrossRef]